

# EVA hot-melt adhesive with thermoplastic starch blends compatibilized by modified maleic anhydride

Larissa Takigava Acrani<sup>1\*</sup>  and Antonio José Felix Carvalho<sup>1</sup> 

<sup>1</sup>*Escola de Engenharia de São Carlos, Universidade de São Paulo - USP, São Carlos, SP, Brasil*

\*[larissatacrani@gmail.com](mailto:larissatacrani@gmail.com)

## Abstract

Hot melt adhesives based on blends of poly (ethylene-co-vinyl acetate), (EVA), and thermoplastic starch modified with citric acid (TPS), compatibilized with polyolefin grafted with maleic anhydride (PO-g-MA) were prepared. The materials were characterized by scanning electron microscopy (SEM) of fragile fractured surface, rotational viscosimeter (Brookfield) and FTIR. SEM showed interfacial failure in non-compatibilized blends and a decrease in the size of TPS dispersed phase as compatibilizer is added. When adding 5 and 7% of the compatibilizer, results from the viscosimeter indicated increase of 85% and 109% in viscosity, respectively. FTIR showed a dislocation in the absorption of hydrogen bands and ester linkages. These results indicated the effectiveness of the polyolefin functionalized. In performance analysis, compatibilized blends with 25% TPS, exhibited greater adhesion compared to standard hot melt adhesive at low application temperature (140°C), which demonstrates great potential for natural materials in adhesive's industry.

**Keywords:** *adhesion, blends, hot-melt adhesive, thermoplastic starch.*

**Data Availability:** Research data is available upon request from the corresponding author.

**How to cite:** Acrani, L. T., & Carvalho, A. J. F. (2025). EVA hot-melt adhesive with thermoplastic starch blends compatibilized by modified maleic anhydride. *Polímeros: Ciência e Tecnologia*, 35(4), e20250038. <https://doi.org/10.1590/0104-1428.20240105>

## 1. Introduction

Adhesives play a crucial role in society with application in a wide range of materials<sup>[1,2]</sup>. Due to their versatile functionality and multidisciplinary applications, adhesives are utilized across various industries such as wood processing, furniture, construction, aerospace, automotive, electronics, packaging and medical applications<sup>[1-5]</sup>. Each of these applications has its own unique requirements and specific characteristics.

In recent years, driven by growing environmental awareness and regulations, the entire chemical industry has focused on improve the sustainability of process and products<sup>[6]</sup>. For adhesives segment, this shift has mostly exhibited in the transition from solvent-based to water-based or 100% solid content adhesives, such as hot melt adhesives<sup>[6,7]</sup>.

Hot melt adhesives (HMA) were introduced in the market in 1950, and have steadily gained significance, now occupying approximately 15 – 21% of the adhesives segment<sup>[8]</sup>. This substantial share is attributed to several factors, such as the absence of solvent in their formulation, allowing for application in high-speed machines<sup>[9]</sup> and their role in addressing environmental concerns regarding volatile organic compounds (VOC) emissions<sup>[10]</sup>. Even though substantial progress has been made, there still a long way to go in the adhesive industry. Notably, most of their raw materials are derived from petroleum sources, which are in predominantly non-biodegradable and non-recyclable<sup>[11]</sup>.

Given the issue with petroleum feedstock and the associated environmental concerns, studies have been

exploring more sustainable alternatives for raw materials in adhesives. The most intuitive path involves natural renewable polymers that already possess natural adhesion characteristics, such as starch (a polysaccharide) and casein (a protein)<sup>[6,10]</sup>. Starch serves as the primary source of energy to sustain life and is a great promise for biopolymers, because of its versatility, low cost, and abundance<sup>[7,12]</sup>. In addition, it can be transformed into a thermoplastic material, known as TPS, by processing in the presence of plasticizers such as glycerol under high temperature, pressure, and shear forces<sup>[12]</sup>.

Carvalho et al.<sup>[13]</sup>, developed a thermoplastic starch (TPS) based hot melt adhesive (HMA) with reduced viscosity, achieved through the incorporation of citric acid into the formulation. While the complete biodegradability of such HMAs is highly promising, these materials still present critical limitations for industrial application, particularly regarding water absorption and thermal stability.

To overcome these drawbacks, one promising strategy is blending TPS with synthetic polymers to enhance performance. Among them, poly(ethylene-co-vinyl acetate) (EVA), a widely used polymer in the adhesive industry, has been the focus of numerous studies. TPS/EVA blends have shown encouraging results, such as a 50% reduction in water uptake<sup>[14]</sup>, indicating strong potential for further development<sup>[15]</sup>. However, these studies have focused on simplified binary systems, such as EVA/TPS blends.

In contrast, the present study expands on this by exploring a more complex, multi-component system of an EVA/TPS hot melt adhesive (HMA), incorporating standard HMA components such as waxes and resins, along with polyolefin grafted with maleic anhydride (PO-g-MA) as a compatibilizer.

The blends were characterized by Fourier-transform infrared spectroscopy (FTIR), rotational viscometry, thermal stability analysis, adhesion testing, and scanning electron microscopy (SEM). Despite being less commonly applied to hot melt adhesives, SEM was employed as a complementary technique to investigate morphological aspects related to blend compatibilization.

This study addresses existing gaps in the literature by exploring the application of TPS/EVA blends in more complex hot melt adhesive (HMA) system, incorporating waxes and conventional tackifiers such as rosin ester and hydrocarbon resins. Additionally, it investigates the effects of compatibilization on morphology, viscosity behavior, offering an application-oriented approach to the research of sustainable HMA formulations, highlighting excellent adhesion performance—specially at reduced application temperatures (140 °C)—while also emphasizing the remaining challenges and opportunities for industrial implementation.

## 2. Materials and Methods

### 2.1 Materials

In this study, regular corn starch with an amylose content of approximately 28% was combined with glycerol, citric acid, and stearic acid. The components of the standard hot melt adhesives are detailed in Table 1. Additionally, the specifications of the substrate for the adhesion tests are provided.

### 2.2 Methods of preparation

#### 2.2.1 Preparation of thermoplastic starch (TPS)

The TPS composition consisted of 61% starch, 33% glycerol, 5% citric acid, and 1% stearic acid. The mixture of components was stored overnight before processing. The mixture was passed through a sieve and fed into a single-screw extruder with a screw diameter of 16 mm and an L/D ratio of 26. The temperature profile was 110°C, 120°C, and 130°C from feed to die, and the screw speed was set to 74 rpm.

#### 2.2.2 Preparation of hot melt adhesives (F1 and F2)

For the production of hot melt adhesives, a mechanical system digester was utilized to blend all components. Initially, less viscous materials – wax, resin – were introduced, followed by the addition of the polymers, which is more viscous. Finally, after some homogenization, the antioxidant was added. The operating temperature was maintained at 140°C with a rotor speed of 250 rpm. Two standard formulations of hot melt adhesives were prepared, featuring ingredients as detailed in Table 1. The proportions were: 49% resin, 30% EVA polymer, 20% wax, and 1% antioxidant.

#### 2.2.3 Preparation of the blends

To prepare the blends, the same procedure used to prepare hot melt adhesives was employed, wherein TPS was mixed with the standard hot melt. Taking this into account, the final formulations are presented in Table 2.

Even formulations that incorporate only a fraction of renewable raw materials can represent a significant step toward environmental sustainability—particularly when these formulations maintain performance standards without incurring additional costs<sup>[6]</sup>. The formulated blends explores incorporating 25% thermoplastic starch (TPS), which is a low cost material, in standard industrial formulas of hot melt adhesives.

**Table 1.** Materials of the formula of citric modified starch-EVA based hot melt adhesive.

Samples	Materials
Both formulas F1 and F2	Polymer: EVA(28% of acetate vinyl content, MFI: 400g/10min), Antioxidant: Primary type
F1: Standard hot melt adhesive with hydrocarbon resin	Resin: Hydrogenated hydrocarbon (C5 Aliphatic) Wax: Fischer-Tropsch, Compatibilizer: Polyolefin functionalized with maleic anhydride
F2: Standard hot melt adhesive with ester resin	Resin: Glycerol ester, Wax: Ethene Copolymer EVA Wax (Acetic Acid Ethyl Ester, with 13% Vinyl Acetate)
Carton paper for packaging	Composition: triple-layer coating comprising short and long fiber cellulose, a blend of short and long fiber cellulose with CMTF, and long fiber cellulose enhanced with starch. Grammage 205 to 360 gsm. Cobb value of 40 g H <sub>2</sub> O/m <sup>3</sup>

**Table 2.** Composition of the blends studied, showing thermoplastic starch (TPS), hot melt adhesive (HMA) content and type (F1 or F2 formulation), and the percentage of polyolefin-grafted-maleic anhydride (PO-g-MA) used as compatibilizer (C).

Sample ID	TPS (%)	HMA (%)	Formulations HMA Type	Compatibilizer PO-g-MA (%)
TPS/F1	25	75	F1	0
TPS/F1/5C	25	70	F1	5
TPS/F1/7C	25	68	F1	7
TPS/F2	25	75	F2	0

To overcome the pronounced polarity mismatch between thermoplastic starch (TPS) and low-polarity HMA F1 and its blends, the compatibilizer (C), as known as polyolefin-grafted maleic anhydride (PO-g-MA), was incorporated at varying concentrations (5% and 7%). This formulation strategy enables a targeted assessment of the compatibilizing effect of PO-g-MA in systems with intrinsically poor interfacial affinity. Conversely, no compatibilizer was added to the blend with the F2 system, as the higher polarity of the ester-based tackifiers enhance compatibility with TPS through more favorable intermolecular interactions.

### 2.3 Characterization methods

The base formulation (TPS/F1) and its modified versions containing 5% and 7% PO-g-MA (TPS/F1/5C and TPS/F1/7C) were extensively characterized using FTIR spectroscopy and viscosity analysis. These techniques were applied exclusively to these formulations due to their high sensitivity in detecting molecular interactions and variations in flow behavior induced by the PO-g-MA compatibilizer. All blend formulations, including TPS/F2, were evaluated by SEM, thermal stability, and adhesion testing to assess performance and compare the morphology of the matrix and dispersed phases.

#### 2.3.1 Thermal stability

Thermal stability were performed according to ASTM D4499 – 17. The samples were placed in a preheated oven set to 150 °C and the temperature was monitored and maintained consistently throughout the duration of the test. The samples were then subjected to the specified temperature for a total duration of 3 hours. After the 3-hour heating period, the samples were removed from the oven and allowed to cool to room temperature. The blends were then visually inspected for signs of phase segregation, such as changes in color, texture, and the presence of distinct layers or domains within the samples. Since there was completely phase segregation for all blends the viscosity was measured only before testing.

#### 2.3.2 Scanning Electron Microscopy (SEM)

For the analysis, the samples were cryogenically fractured using liquid nitrogen, coated with a thin layer of platinum, and examined using an Inspect F-50 scanning electron microscope (SEM). This well-established preparation method for polymeric materials was chosen to overcome the inherent softness and low electrical conductivity of the hot melt adhesives.

#### 2.3.3 Fourier Transform Infrared Spectroscopy (FTIR)

The FTIR analysis was performed using a Perkin Elmer Spectrum 3 spectrometer, equipped with an ATR (Attenuated Total Reflectance) module for the measurements. FTIR spectra were recorded in the range of 4000 to 650  $\text{cm}^{-1}$ , with 16 scans per sample.

#### 2.3.4 Viscosity measurement

The viscosity of the blends was measured using a Brookfield viscometer, equipped with spindles 27 and 29. Measurements were taken within the temperature range of 120 to 150 °C, with rotational speeds set at 20, 50, and 100 rpm.

#### 2.3.5 Adhesion testing

The application of adhesives was performed using a Slautterback Mini Squirt II application gun on a standardized rectangular surface measuring 50 mm x 100 mm. To ensure precise bonding, temperatures of 140 °C for TPS blends and 150 °C for standard hot melt adhesives were carefully maintained. Initially, the adhesive was applied to the internal surface of the carton paper, promoting adherence with the external counterpart. After a brief open time of 1 second, a 100 g weight was applied to the substrate for 3 seconds, effectively characterizing the adhesive's setting time. Following a 24-hour period to facilitate bond development, the adhered substrates underwent manual separation using a peel force technique to evaluate adhesion performance, focusing on fiber tear of the substrate. The primary objective was to assess the interaction between the adhesive and the substrate, emphasizing bond effectiveness as demonstrated by fiber tear performance rather than solely measuring the force required to separate the samples.

Following the fiber tear classification method described by Robertson et al. (2021), the bonds were pulled apart after the 24-hour period to evaluate the extent of fiber tear. Five bonds were tested for each adhesive, and an average value was calculated. The averages were classified as follows: 81–100% fiber tear = Full fiber tear; 51–80% fiber tear = Partial fiber tear; 21–50% fiber tear = Slight fiber tear; and 0–20% fiber tear = No fiber tear<sup>[16]</sup>.

## 3. Results and Discussions

### 3.1 Materials characterization

#### 3.1.1 Thermal stability at 150 °C

The thermal stability results obtained of the blends are presented in Figure 1.

The blends exposed for 3 hours at 150 °C exhibited visible phase separation, as illustrated in Figure 1. This phenomenon may be attributed to the disruption of hydrogen bonding within the blend, as well as the coalescence of the dispersed phase, further exacerbated by the low thermal stability of TPS, which promotes rapid phase differentiation from the matrix. Notably, in Figure 1a, the formulation TPS/F1 displayed the most pronounced phase segregation at 150 °C, with the dispersed TPS phase exhibiting a larger domain size due to polarity mismatch with the matrix, F1, demonstrating coalescence effects. Conversely, the results upon the addition of the compatibilizer in Figure 1b and Figure 1c, led to a significant improvement in phase homogeneity, although some degree of segregation persisted. Furthermore, a similar performance was observed for the blend containing ester resin (TPS/F2), Figure 1d when compared to the compatibilized blends shown in Figures 1b, c.

#### 3.1.2 Scanning electron microscopy (SEM) analysis

In the TPS/F1 blend (Figure 2a), only the matrix phase of HMA F1 is visible. According to the literature<sup>[17,18]</sup>, the presence of the TPS phase would typically manifest as a failure characterized by a flat and uniform structure due to brittle fracture associated with the amorphous phase.

This observation suggests that the failures depicted in Figures 2b-d may be attributed to the dispersed TPS phase within the matrix.

In contrast, the morphology observed in the TPS/F1 blend, at Figure 2a, which did not show the presence of TPS, may result from the macroscopic phase segregation within the mixture, likely due to low compatibility between TPS and HMA F1. The addition of a compatibilizer significantly improved the interfacial interactions between the phases, as demonstrated in the blends TPS/F1/5C (Figure 2c) and TPS/F1/7C (Figure 2d). In these modified blends, the presence of voids indicates

the detachment of the TPS dispersed phase, which is a result of adhesion failure.

Furthermore, as the proportion of the compatibilizer, functionalized polyolefin increased (PO-g-MA), a corresponding decrease in particle diameter was observed, indicating a reduction in interfacial tension between the phases, as shown in Figure 2c and Figure 2d. These results align with expectations, as the compatibilizer effectively reduces interfacial tension between the components, thereby increasing adhesion energy and stabilizing their morphology<sup>[19,20]</sup>. Consequently, this leads to a decrease in the particle diameters of the dispersed phases.

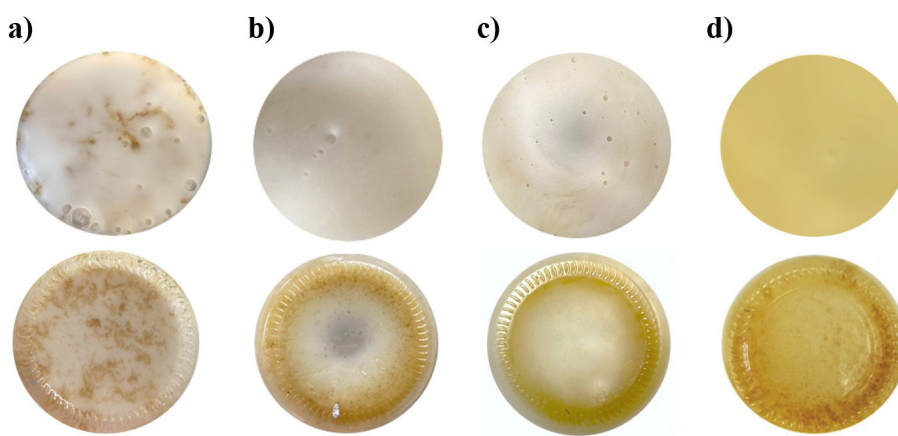


**Figure 1.** Thermal stability of blends (a) TPS/F1, (b) TPS/F1/5C, (c) TPS/F1/7C, (d) TPS/F2.

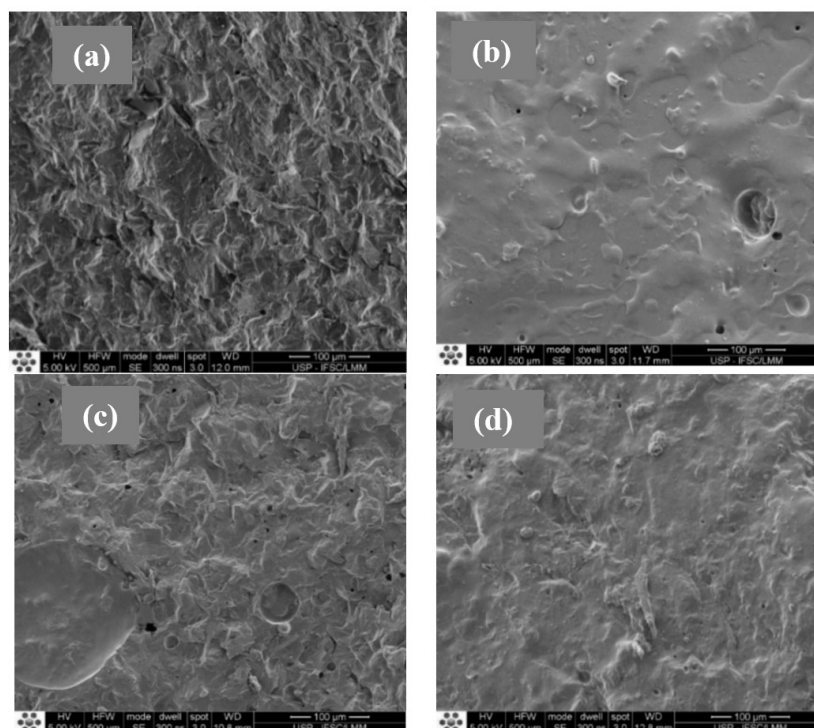


**Figure 2.** SEM images of fragile fracture surfaces of the blends (a) TPS/F1, (b) TPS/F2, (c) TPS/F1/5C, and (d) TPS/F1/7C.

## 3.1.3 Fourier Transform Infrared Spectroscopy (FTIR)

The resulting blends with EVA hot-melt adhesive F1, with thermoplastic starch (TPS) are presented in Figure 3 and Figure 4 for the following formulations: (a) TPS/F1, (b) TPS/F1/5C, and (c) TPS/F1/7C. Figure 3a-c provides a comparative overview of the FTIR spectra of the blends against their individual components—namely (d) F1, (e) the compatibilizer PO-g-MA, and (f) TPS. In contrast, Figure 4 offers a more detailed analysis of the absorption bands corresponding to functional groups within the blends, revealing the differences between them and how they result

from the molecular structures of the individual components in Figure 3d-f.

The absorption bands observed in Figure 4a-c can be primarily correlated with the spectra of HMA F1 in Figure 3d and TPS in Figure 3f, as they are the major components of the blends. Due to the low concentration of the compatibilizer (PO-g-MA), it is not possible to clearly identify its characteristic absorption bands in Figure 4a-c based on the spectrum shown in Figure 3e. However, its influence on the blend's properties will be further discussed in Figure 5.

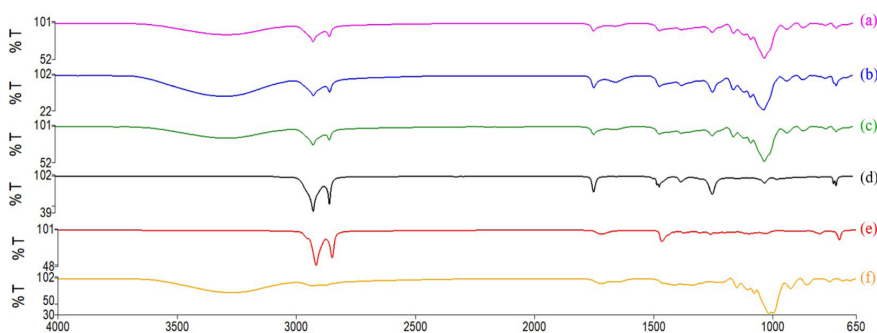


**Figure 3.** FTIR of EVA Hot-Melt Adhesive with Thermoplastic Starch Blends (a) TPS/F1 (b) TPS/F1/5C (c) TPS/F1/7C and their individual components (d) F1 (e) Compatibilizer PO-g-MA (f) TPS.

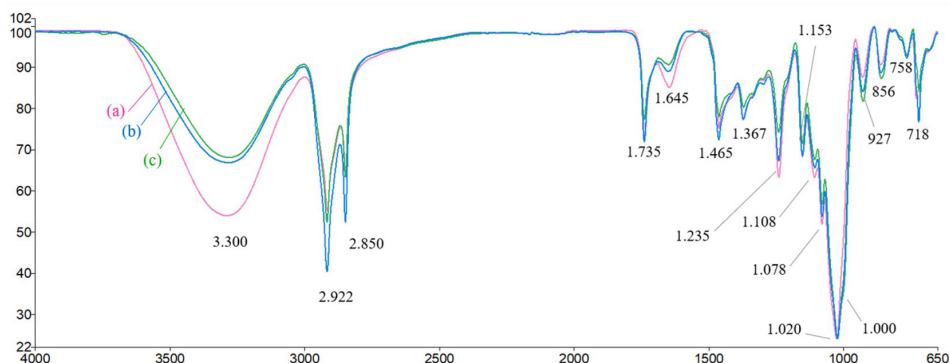


**Figure 4.** FTIR spectra with band assignments for the following blends (a) TPS/F1, (b) TPS/F1/5C (c) TPS/F1/7C

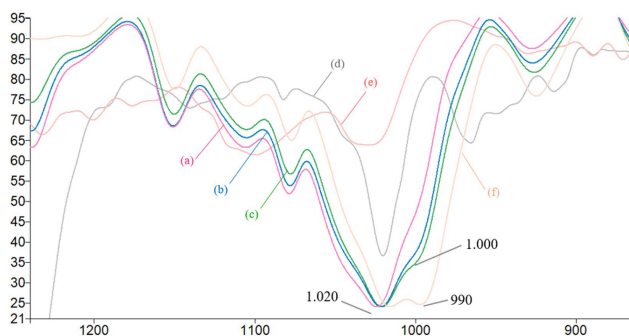


**Figure 5.** Comparison of the blends (a) TPS/F1 (b) TPS/F1/5C (c) TPS/F1/7C and their individual components (d) F1 (e) Compatibilizer PO-g-MA (f) TPS in the region between 990 to 1.020  $\text{cm}^{-1}$  highlighting band dislocations.

Characteristic absorptions from the HMA F1 are clearly identified in Figure 4a-c, such as the C–H asymmetric and symmetric stretching vibrations at 2922 and 2850  $\text{cm}^{-1}$ , respectively. Bending vibrations of methylene groups ( $-\text{CH}_2-$ ) are also evident at 1465  $\text{cm}^{-1}$ . These absorptions can be attributed to multiple constituents of the HMA F1, including hydrogenated hydrocarbon resins, paraffin wax, and EVA copolymer itself. Additionally, ester groups specific to poly(ethylene-co-vinyl acetate) (EVA) are observed at 1735  $\text{cm}^{-1}$  (C=O stretching) and 1235  $\text{cm}^{-1}$  (C–O stretching)<sup>[21]</sup>.

Furthermore, functional groups associated with TPS are also clearly present in Figure 4a-c. A broad and intense O–H stretching vibration appears at 3300  $\text{cm}^{-1}$ , along with a weaker band at 1645  $\text{cm}^{-1}$ . Notably, the region from 1235 to 650  $\text{cm}^{-1}$  in Figure 3a-c and Figure 4a-c closely resembles that of pure TPS from Figure 3e. In this region, C–O stretching vibrations from the glucopyranose ring are observed at 1077 and 858  $\text{cm}^{-1}$ . Additional bands at 1153 and 927  $\text{cm}^{-1}$  are attributed to C–O vibrations associated with  $\alpha$ -1,4 glycosidic linkages. A prominent doublet between 1020 and 990  $\text{cm}^{-1}$  is also evident, corresponding to the stretching of C–OH groups<sup>[21]</sup>.

Figure 5 presents a more detailed analysis of the two most intense absorption bands in the blends, originally assigned to TPS at 1013  $\text{cm}^{-1}$  and 990  $\text{cm}^{-1}$ , from Figure 5f, both associated with C–OH stretching vibrations. In the blends, these bands show noticeable dislocations to 1020 and 990  $\text{cm}^{-1}$ , respectively. However, for the uncompatibilized blend (TPS/F1) shown in Figure 5a, the second absorption band at 990  $\text{cm}^{-1}$  is nearly absent.

Upon incorporating the compatibilizer PO-g-MA (polyolefin grafted with maleic anhydride) at concentrations of 5% and 7%, the FTIR spectra of the compatibilized blends TPS/F1/5C and TPS/F1/7C show a significant increase in band intensity around 1000  $\text{cm}^{-1}$  at Figure 5b, c, with increasing PO-g-MA concentration. In contrast, this band was barely detectable in the uncompatibilized blend (TPS/F1) in Figure 5a. The enhanced intensity indicates stronger intermolecular interactions, contributing to improved interfacial compatibility and adhesion between the polar TPS and the nonpolar EVA-based HMA matrix of F1. This result supports the role of PO-g-MA as an effective compatibilizer, enhancing molecular affinity and dispersion at the interface.

Furthermore, as shown in Figure 4a-c, the addition of the compatibilizer leads to a significant decrease in the intensity of the hydroxyl stretching vibrations at 3300 and 1645  $\text{cm}^{-1}$ , which becomes more pronounced with increasing amounts of PO-g-MA. This reduction in band intensity may indicate a lower concentration of free hydroxyl groups from TPS, likely due to interactions with the maleic anhydride groups.

This suggests improved incorporation of the dispersed TPS phase into the HMA F1 matrix, highlighting the strong compatibilizing effect of PO-g-MA.

### 3.1.4 Viscosity analysis

The results of viscosity measurement for the adhesives are presented in Table 3.

The sample of thermoplastic starch blended with the standard hot melt containing hydrogenated hydrocarbon resin (TPS/F1) exhibited a viscosity comparable to that of the pure HMA formula (F1). In the evaluation of other blends (TPS/F1/5C, TPS/F1/7C), it was observed that as the proportion of the compatibilizer increased, the viscosity also rose significantly. These findings are consistent with the results from the SEM and FTIR analysis, which demonstrate the compatibilizer's effectiveness in enhancing compatibilization and reducing surface energy at the interface of the samples. This effect likely facilitates the formation of entanglements, as polymer chain entanglements typically lead to an increase in molar mass and, consequently, an increase in the viscosity of the final polymeric mixture<sup>[22]</sup>.

### 3.1.5 Adhesion tests

The blend (TPS/F1) exhibited adhesion failure, resulting in 0% fiber tear, mirroring the performance of the standard HMA F1 formula, as shown in Figure 6a and 6e. This inadequate performance can be attributed to several interconnected factors: the application temperature of the standard formula was set at 140 °C, which is lower than the optimal range typically required for strong adhesive bonding, potentially leading to insufficient wettability and coverage; phase segregation within the blend may have occurred due to inadequate compatibility between the TPS and HMA components, resulting in weak regions that contribute to failure; additionally, the challenges of adhering to carton paper substrates—characterized by a smoother surface and lower surface energy compared to corrugated paper—further hinder effective bonding.

In contrast, blends incorporating thermoplastic starch (TPS) and polyolefin functionalized with maleic anhydride (PO-g-MA), as TPS/F1/5C and TPS/F1/7C, demonstrated great adhesion at 140 °C, as illustrated in Figure 6b and 6c, with fiber tear exceeding 90%. Furthermore, Figures 6d and 6f showcased excellent performance, achieving 100% fiber tear for both HMA F2 and the blend TPS/F2.

The results of these blends highlight the effectiveness of the formulations in achieving robust adhesion, even at lower application temperatures. The incorporation of polyolefin functionalized with maleic anhydride (PO-g-MA) significantly enhances the adhesive properties by improving compatibilization between the adhesive matrix and the substrate.

**Table 3.** Viscosity Behavior of HMA F1 Blends as a Function of PO-g-MA Concentration

Samples ID	120 °C	130 °C	140 °C	150 °C
F1	4.000	2.625	1.875	1.350
TPS/F1	4.800	2.850	2.100	-
TPS/F1/5C	8.900	5.400	3.250	-
TPS/F1/7C	10.020	6.740	4.440	-

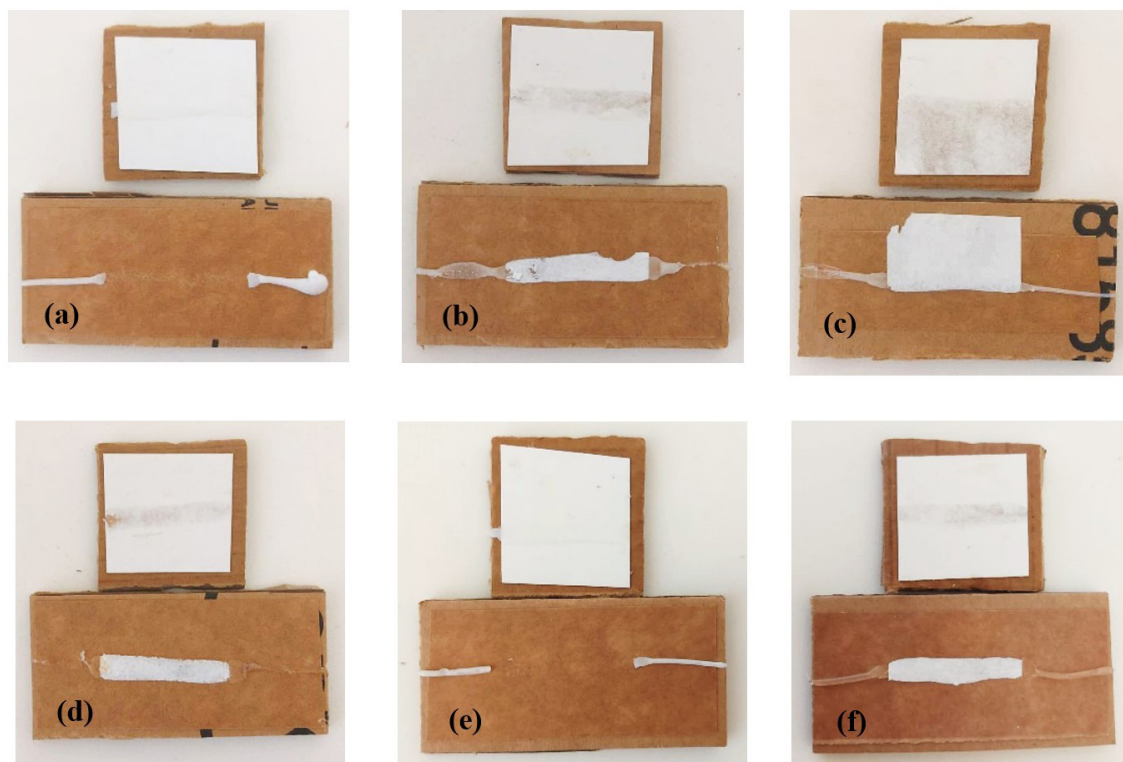


**Figure 6.** Results of adhesion, (a) TPS/F1, (b) TPS/F1/5C, (c) TPS/F1/7C, (d) TPS/F2, (e) F1 (f) F2.

This enhanced interaction leads to increased adhesion strength and overall performance, particularly when combined with thermoplastic starch, which also contributes to adhesion enhancement through its cohesive properties.

Furthermore, these formulations demonstrate excellent interaction with the evaluated carton paper, which has starch on its surface. This compatibility is pivotal in explaining the superior performance of blends containing TPS, as it fosters improved bonding at the interface. In summary, the integration of thermoplastic starch and polyolefin functionalized with maleic anhydride not only enhances adhesion performance but also optimizes compatibility with the substrate. This results in superior adhesive properties, particularly at application temperatures as low as 140 °C.

#### 4. Conclusions

The results demonstrate the significant potential of thermoplastic starch (TPS) as an adhesive at low application temperatures. One promising strategy to enhance the compatibility of TPS with non-polar materials, such as those found in standard hot melt adhesive formulations, is the use of polyolefins functionalized with maleic anhydride (PO-g-MA). The incorporation of PO-g-MA helps reduce phase separation and enhances compatibility between the polyolefin matrix and the dispersed TPS phase, demonstrating a synergistic approach. Beyond its sustainability benefits, TPS also improves adhesive performance, as shown by adhesion tests on carton paper, and delivers superior bonding properties at lower application temperatures.

However, to successfully introduce green adhesives into the market, key advancements are needed, particularly in improving thermal stability, which plays a crucial role in industrial machinability. Additionally, natural polymer blends with ester resins present an intriguing opportunity due to their renewable origin, polar functional groups, and the availability of high-quality variants specially in Brazil, which compatibilization techniques with this resin wasn't further explored in this article. In conclusion, while TPS-based adhesives, also natural polymers adhesives show considerable promise for adhesion industry, further research is required to address thermal stability, compatibility and processing challenges to unlock their potential in industrial applications.

#### 5. Author's Contribution

- **Conceptualization** – Larissa Takigava Acrani; Antonio José Felix Carvalho.
- **Data curation** – Larissa Takigava Acrani.
- **Formal analysis** – Larissa Takigava Acrani, Antonio José Felix Carvalho.
- **Funding acquisition** – Antonio José Felix Carvalho.
- **Investigation** – Larissa Takigava Acrani
- **Methodology** – Larissa Takigava Acrani; Antonio José Felix Carvalho.
- **Project administration** – Larissa Takigava Acrani.
- **Resources** – Larissa Takigava Acrani; Antonio José Felix Carvalho.

- **Software** – NA.
- **Supervision** – Antonio José Felix Carvalho.
- **Validation** – Larissa Takigava Acrani.
- **Visualization** – Larissa Takigava Acrani.
- **Writing – original draft** – Larissa Takigava Acrani.
- **Writing – review & editing** – Larissa Takigava Acrani; Antonio José Felix Carvalho.

## 6. Acknowledgements

The authors would like to acknowledge Research and Development & Application Engineering Department of Henkel Ltda, Jundiaí, SP/Brazil. Antonio J. F. Carvalho is CNPq fellow (Number: 308709/2023-3).

## 7. References

1. Ma, Y., Kou, Z., Hu, Y., Zhou, J., Bei, Y., Hu, L., Huang, Q., Jia, P., & Zhou, Y. (2023). Research advances in bio-based adhesives. *International Journal of Adhesion and Adhesives*, 126(4), 103444. <http://doi.org/10.1016/j.ijadhadh.2023.103444>.
2. Pereira, A. B., & Pereira, A. L. (2023). *Introductory chapter: the importance of adhesives in the world*. In L. Li, A. B. Pereira, & A. L. Pereira (Eds.), *Next generation fiber-reinforced composites – New insights*. IntechOpen. <http://doi.org/10.5772/intechopen.108295>.
3. Arias, A., González-García, S., González-Rodríguez, S., Feijoo, G., & Moreira, M. T. (2020). Cradle-to-gate Life Cycle Assessment of bio-adhesives for the wood panel industry. A comparison with petrochemical alternatives. *The Science of the Total Environment*, 738, 140357. <http://doi.org/10.1016/j.scitotenv.2020.140357>. PMID:32806374.
4. Emblem, A., & Hardwidge, M. (2012). *Adhesives for packaging*. In A. Emblem, & M. Hardwidge (Eds.), *Packaging Technology – Fundamentals, materials and processes* (pp. 381-394). Sawston: Woodhead Publishing.
5. Webster, I., & West, P. J. (2001). *Adhesives for medical applications*. In S. Dumitriu (Eds.), *Polymeric biomaterials, revised and expanded* (pp. 717-752). Boca Raton: CRC Press. <http://doi.org/10.1201/9780203904671.ch26>.
6. Heinrich, L. A. (2019). Future opportunities for bio-based adhesives – advantages beyond renewability. *Green Chemistry*, 21(8), 1866-1888. <http://doi.org/10.1039/C8GC03746A>.
7. Frihart, R. C., Hunt, C. G., & Birkeland, M. J. (2013). *Soy Proteins as Wood Adhesives*. In W. Gutowski, & H. Dodiuk (Eds.), *Recent Advances in Adhesion Science and Technology in Honor of Dr. Kash Mittal* (pp. 277-291). Boca Raton: CRC Press.
8. Khairullin, I. K. (2013). Adhesive-melts-the most dynamically developing area in world production and consumption of adhesives. *Polymer Science, Series D. Glues and Sealing Materials*, 6(1), 77-81. <http://doi.org/10.1134/S1995421213010073>.
9. Paul, C. W. (2002). *Hot melt adhesives*. In D. A. Dillard, A. V. Pocius, & M. K. Chaudhury (Eds.), *Adhesion science and engineering* (pp. 711-757). USA: Elsevier Science B. V.
10. Vineeth, S. K., & Gadhave, R. V. (2020). Sustainable raw materials in hot melt adhesives: a review. *Open Journal of Polymer Chemistry*, 10(3), 49-65. <http://doi.org/10.4236/ojpcem.2020.103003>.
11. Li, W., Bouzidi, L., & Narine, S. S. (2008). Current research and development status and prospect of hot-melt adhesives: a review. *Industrial & Engineering Chemistry Research*, 47(20), 7524-7532. <http://doi.org/10.1021/ie800189b>.
12. Carvalho, A. J. F. (2008). *Starch: major sources, properties and applications as thermoplastic materials*. In M. N. Belgacem, & A. Gandini (Eds.), *Monomers, polymers and composites from renewable resources* (pp. 321-342). USA: Elsevier Science. <http://doi.org/10.1016/B978-0-08-045316-3.00015-6>.
13. Carvalho, A. J. F. (2010). *Processo para a preparação de adesivo aplicado por aquecimento (cola quente ou hot melt) biodegradável a base de amido termoplástico* (Patente BR PI 1005124-4 A2). Universidade Federal de São Carlos – UFSCar, Brasil.
14. Da Róz, A. L., Ferreira, A. M., Yamaji, F. M., & Carvalho, A. J. F. (2012). Compatible blends of thermoplastic starch and hydrolyzed ethylene-vinyl acetate copolymers. *Carbohydrate Polymers*, 90(1), 34-40. <http://doi.org/10.1016/j.carbpol.2012.04.055>. PMID:24751007.
15. Patel, V. (2009). Preparation and Characterization Of Biodegradable and Compatible Ethylene Vinyl Acetate (EVA)/ Thermoplastic Starch (TPS) Blend Nanocomposites. *Advanced Materials Research*, 67, 185-189. <http://doi.org/10.4028/www.scientific.net/AMR.67.185>.
16. Robertson, D., Van Reenen, A. J., Duveskog, H., & Brady, F. (2021). A comparative study of the application-based properties of hot melt adhesives (HMAs) formulated with different waxes. *International Journal of Adhesion and Adhesives*, 111, 102974. <http://doi.org/10.1016/j.ijadhadh.2021.102974>.
17. Miranda, V. R., & Carvalho, A. J. F. (2011). Blendas compatíveis de amido termoplástico e polietileno de baixa densidade compatibilizadas com ácido cítrico. *Polímeros: Ciência e Tecnologia*, 21(5), 353-360. <https://doi.org/10.1590/S0104-14282011005000067>.
18. Oliveira, C. F. P. (2022). *Obtenção e caracterização de amido termoplástico e de suas misturas com polipropileno* (Doctoral dissertation). Escola Politécnica, Universidade de São Paulo, São Paulo.
19. Utracki, L. A. (2022). Compatibilization of polymer blends. *Canadian Journal of Chemical Engineering*, 80(6), 1008-1016. <http://doi.org/10.1002/cjce.5450800601>.
20. Thumber, C. M. (2015). *Compatibilization of polyolefin blends* (Doctoral dissertation). University of Minnesota, Minnesota, USA.
21. Pavia, D. L., Lampman, G. M., Kriz, G. S., & Vyvyan, J. A. (2008). *Introduction to spectroscopy*. Boston: Cengage Learning.
22. Bretas, R. E. S., & D'Ávila, M. A. (2006). *Reologia de polímeros fundidos*. São Carlos: Edufscar.

Received: Jan. 02, 2025

Revised: May 02, 2025

Accepted: Jun. 16, 2025

Editor-in-Chief: Sebastião V. Canevarolo